doi.org/10.36721/PJPS.2024.37.5.REG.1151-1161.1

Novel pyrimidine derivatives and black cumin as xanthine oxidase inhibitors: Synthesis, docking study and formulation

Salam Waheed Ahjel[1], Suhad Sami Humadi[1], Samir Mohamed Awad[1,2], Mohamed Fathy El-Shehry[1,3*], Yara Essam Mansour[2] and Ahmed Abd Elkader El-Rashedy[4]

[1]Pharmacy Department, Al-Zahrawi University College, Karbala, Iraq
[2]Pharmaceutical Organic Chemistry, Faculty of Pharmacy, Helwan, Egypt
[3]Pesticides Chemistry Department, National Research Centre, Dokki, Giza, Egypt
[4]Chemistry of Natural and Microbial Products, National Research Centre, Dokki, Giza, Egypt

Abstract: In this work, to attempt discovery of novel xanthine oxidase (XO) inhibitors, we developed a method for optimizing the Nigella sativa oil extraction by considering the seed size particles, the liquid seed ratio, the duration of the extraction procedure and the temperature of extraction. On the other hand, new pyrimidine and triazolopyrimidine derivatives were prepared in an attempt to mimic the pyrazolpyrimidine structure of allopurinol (a well-known xanthine oxidase inhibitor drug). Most of the developed compounds were shown to have strong xanthine oxidase inhibitory activities, while Nigella sative extract and compound 6b ranked as the most effective inhibitors (IC_{50}=1.87 and 0.63µg/ml, respectively, versus Allupurinol's IC_{50}=0.62µg/ml). Nigella sative extract and compound 6b showed potent activity (IC_{50}=0.60µg/ml). In addition, compound 6b was formulated as effervescent granules and exhibited good flow-ability properties. To further understand the approach of binding between synthesized compounds 6a-c and xanthine oxidase, a molecular docking investigation was conducted. These findings highlight the discovery of a novel group of xanthine oxidase inhibitors with the potential to improve the state-of-the-art treatment for gout.

Keywords: Black seed, pyrimidine and triazolopyrimidines, xanthine oxidase inhibitors, effervescent granules, docking study.

Submitted on 15-06-2023 – Revised on 05-10-2023 – Accepted on 05-10-2023

INTRODUCTION

The purine metabolic illness syndrome known as hyperuricemia can be caused on by either an inadequate elimination of uric acid or an excessive production of uric acid. Both gouty arthritis and hyperuricemia are conditions that are brought on by an overabundance of uric acid in the joints and bones (Liu *et al.,* 2021).

Hypoxanthine and xanthine are converted to uric acid (UA) by the enzyme xanthine oxidase (XO), which is found mostly in the liver, kidneys and vascular endothelium (Battelli *et al.,* 2016) clusters and a flavin adenine dinucleotide center domain; total molecular weight is 290 kilodaltons (Enroth *et al*., 2000). The molybdenum core is particularly important for controlling the breakdown of natural purines (Okamoto *et al*., 2013). Because of its potential role in pathological UA overproduction, XO has emerged as a focus of intense research and critical importance in the management of hyperuricemia and gout (Ojha *et al*., 2017).

The FDA approved allopurinol to treat gouty arthritis in 1966, however it came with a host of unwanted consequences such hypersensitivity syndrome, liver damage, Stevens-Johnson syndrome and renal toxicity (Hammer *et al*., 2001; Horiuchi *et al*., 2000). Up to now, Allopurinol, febuxostat and topiroxostat, three medicines that target XO, have been approved (Abdizadeh *et al*., 2020). However, these candidates had significant problems that were only discovered after clinical use (fig. 1).

Researchers have made significant attempts to identify novel and powerful XO inhibitors in nature due to the potential benefits of the safety and structure variety of natural molecules compared to synthetic structures (Dzobo *et al*., 2022).

Medical science today is taking a keener interest in traditional practices like employing medicinal herbs for illness prevention and treatment. Nigella sativa (NS), traditional medicine places significant importance on the black seed, also known as black caraway, kalonji, nigella and black cumin (Ahmad *et al*., 2013).

Black cumin, a member of the Ranunculaceae family, has a high concentration of bioactive chemicals and several useful medical applications. Its natural habitats are in southern Europe, northern Africa and south-western Asia. It is currently grown commercially in a number of nations across the globe, including those in the Mediterranean, the Middle East and South Europe; however, the largest producers are the countries of India, Pakistan, Syria, Turkey and Saudi Arabia (Kooti *et al*., 2016). Since the climate in Egypt is ideal for growing *Nigella sativa*, the

*Corresponding author: e-mail: moh_elshehry2000@yahoo.com

country's seeds are among the best available. According to the slogan, "in every condition except death," they were a miracle drug. Nigella sativa has been shown to have therapeutic properties against inflammation, allergies, cancer, high blood pressure, high cholesterol, gout, rheumatoid arthritis and even as a diuretic and kidney protector (Jaarin *et al*., 2015; Zielińska *et al*., 2021; Habibeh *et al*., 2020). Asthma isn't the only condition it helps, though; it can also treat acne and menstrual cycle abnormalities. The neuroprotective effects of Nigella sativa have also been shown in animal models of neurodegenerative disorders such Alzheimer's, Parkinson's, depression and epilepsy (Samarghandian *et al*., 2018; Cobourne-Duval *et al*., 2018).

As a result of allupurinol's restrictions and other medications' side effects, there is a growing interest in discovering novel pharmaceuticals having Xo inhibition action through either natural or synthetic means. The anti-inflammatory properties of black seed oil, combined with its high concentrations of flavonoids, tannins, 15 essential amino acids and others, have been shown to reduce serum uric acid levels and, by extension, the inflammations caused by gouty arthritis. These constituents include thymoquinone, nigellicine, thymohydroquinone, nigellone, nigellidine, nigellimine-N-oxide, dithymoquinone (Horiuchi *et al*., 2000; Razavi *et al*., 2007). In addition, many thiopyrimidine-5-carbonitrile were synthesized because of their wide range of biological applications (Fathalla *et al*., 2007; Mohamed *et al*., 2011).

We have rationally constructed an entirely novel category of hybrid chemical structure by studying the binding of the febuxostat skeleton within the protein pocket. The skeleton's arrangement of triazolopyrimidone and heterocyclic ring (2-thiazolyl, 3-thiazolyl, or thiophenopyridyl) mimics and enhances the interactions found in the febuxostat binding site. In order to achieve this goal, febuxostat has been fragmented into two parts, which are: Part A, which consists of the thiazolenucleus and carboxylic group; Part B, which consists of the aromatic nucleus attached to the isobutane group. The use of cyanotriazolo-pyrimidone in place of Part A resulted in much enhanced interactions when compared to febuxostat. These interactions included four characteristic hydrogen bond interactions: two with Arg880, one with Thr1010, in addition to one extra with Val1011 that is absent in febuxostat itself. In a similar manner, the aromatic nucleus that is connected to the isobutane group of Part B is changed to a different heterocyclic ring that has been embedded within the hydrophobic cleft. This ring could be 2-thiazolyl, 3-thiazolyl, or thiophenopyridyl. The efficacy of the modified cyanotriazolo-pyrimidone moiety in maintaining the essential contact at the active site of xanthine oxidase is great (fig. 2).

This research aims to synthesize and characterize pyrimidine and triazolpyrimidine derivatives linked 2-thiazolyl, 3-thiazolyl, or thiophenopyridyl hybrids in addition to extracting black seed oil and evaluating them for xanthine oxidase inhibitory potential. Since there is a worldwide shortage of xanthine oxidase inhibitors, effective and safer ones are urgently required. Enzyme kinetic investigations were also conducted on all of the molecules. Additionally, molecular docking simulations were run in order to investigate the binding interactions of the most active molecules within the active sites versus febuxostat (a co-crystallized molecule).

MATERIALS AND METHODS

Nigella sativa seeds came from an herbal store in the neighborhood of Hawamdia in the city of Giza in Egypt. Twenty days were spent storing the seeds in the dark at 4ºC. The seeds were blended into a powder of about 150 g in size just before being used in the extraction procedure. Extraction began according to the reported method (Wang *et al.,* 2008).

Instruments

All melting points were measured in Electrothermal IA 9100 equipment from Shimadzu, Japan and are presented here without any corrections. The IR spectra were captured using Perkin-Elmer 1650 spectrophotometer (USA) using potassium bromide pellets. Using tetramethylsilane (TMS) as an internal standard, ^{1}HNMR, on Jeol 500MHz spectrometer and^{13}CNMR, on Bruker 125 MHz NMR spectrometer spectra were performed in DMSO-d_6 (^{1}H) and (^{13}C) instruments, chemical shifts (δ) were stated in ppm. The Shimadzu Ms-QP 1000 (70 ev, EI, Japan) was used to capture the mass spectrum data. The Elementarvario (Shimadzu) equipment was used to conduct the microanalyses. TLC was used to track the development of all of the reactions, with chloroform-methanol (3:1) as the mobile phase and spots being seen by iodine vapors or UV-light (254nm).

Methodology

General procedure for synthesis of 4-oxo-6-aryl-2-thioxo-1,2,3,4-tetrahydropyrimidine-5-carbonitrile (4a-c)

Adding equimolar of ethylacetoacetate (0.01mole), thiourea and the appropriate aldehydes (3a-c) namely; thiazole-2-carbaldehyde, 6-thiophen-3-yl-pyridine-2-carbaldehyde and thiazole-4-carbaldehydestirred in 50 ml ethanol for 4hours in presence of sodium ethoxide at ambient temperature, the workup done in water with diluted HCl, the final solid crystallized using DMF and water.

General procedure for synthesis of 2-hydrazino-4-oxo-6-aryl-1,4-dihydropyrimidine-5-carbonitrile 5a-c

A solution of 4a-c (0.05 mole) and hydrazine hydrate 99% (0.05 mole) refluxed in ethanol (30 ml) for 16 hour, after

completion the reaction worked up with water, the solid crystallized using DMF and water.

General procedure for synthesis of 7-aryl-5oxo-1,5-dihydro[1,2,4] triazolo[4,3-a] pyrimidine-6-carbonitrile (6a-c)

A solution of 5a-c (0.001 mole) refluxed in formic acid (10ml) for 10 hours, the reaction mixture worked up in water and the solid crystallized from DMF and water.

In vitro-antixanthine oxidase assay: reported (Trunghu et al., 2016)

Both black seed extract and all synthesized pyrimidine and triazolopyrimidine derivatives were evaluated with xanthine oxidase inhibition activity. Inhibition of XO due to uric acid production from xanthine was measured using UV-Vis spectroscopy at 296 nm. The technique called for the inclusion of 0.5ml of each examined chemical in DMF, 0.78 ml of phosphate buffer (pH 7.8) and 0.08 ml of bovine milk xanthine oxidase (sigma-Aldrich, USA) that had been newly produced. Each test solution was incubated at R.T for 20 min. The substrate solution was introduced at a volume of 0.67 ml and the reaction proceeded. The absorbance was measured at 296 nm using a UV-Vis spectrometer (1601UV,Shimadzu, Australia) after incubating the assay mixture at 25ºC for 15 minutes and then adding 0.2 ml of 0.5 N HCl to stop the reaction. Allopurinol, a well-established XO inhibitor, served as a reference standard in this inhibition analysis. A comparison to the control sample without inhibitor allowed us to determine the residual activity. Standard deviation was determined by performing the experiment three times. The half-inhibitory concentration (IC_{50}) was calculated by testing various concentrations of the substance against the maximum activity.

Seed extract

Due to the great and versatile medicinal importance of black seeds, many were interested in extraction of the oil and thymoquinone (the main bioactive agent). Many methods of extraction were adopted. Cold pressing is a technique where seeds are pressed at room temperature and the oil is then collected, filtered through Watmannn No.4 and then yielded at a relatively low 27% (Kiralan *et al*., 2014). Furthermore, Dinagaran *et al*. reported a technique for extracting the oil utilizing a soxhlet apparatus with n-hexane as the solvent, achieving a mediocre yield of 29.9% with solvent residues (Dinagaran *et al*., 2016). Kokoska *et al*. utilized a water holding flask in which they placed powdered seeds and a Clevenger type equipment in which the flask was directly linked to the condenser; this basic approach is called hydro distillation. Continuous processing for 2 hours resulted in a poor yield of pale yellow oil (0.29% wt/wt) (Kokoska *et al*., 2008). Also, (Abedi *et al*., 2017) developed Microwave-Assisted extraction method through a domestic microwave oven but only 0.33% essential oil yield was obtained. Other novel methods were used such as Ultrasound-Assisted extraction and steam distillation (Moghimi *et al*., 2018; Sabriu-Haxhijaha *et al*., 2020; Ahmad *et al*., 2020). Perhaps the most modern and efficient method is the supercritical fluid extraction method.

Supercritical Fluid Extraction (SFE)

For the extraction, a German-made Suprex MPS/225 system was used. Under 400 atm. pressures and 40ºC temperature, 15 static minutes and 20 dynamic minutes were spent extracting 150.0g of the totally crashed seeds using the SFE technique. The SFE system utilized a Dura flow manual variable restrictor (Suprex) for sample collection. Through the Duraflow restrictor, the compressed SFE flow rate was around 25g/min. In a volumetric flask, the analytes from the extract were gathered. After the extraction was complete, the volume was brought to 35ml. During the dynamic extraction phase, the 35ml volumetric flask was chilled in an ice bath for optimal collection efficiency.

Formulation of 6b as effervescent granules: (Al-Mousawy et al., 2019; Patel et al., 2016)

Difficulties in water solubility is a main problem in formulation of prepared trizolopyrimidine derivatives, one a suggested method to overcome these difficulties is the preparation of effervescent granules from a combined formula of citric, tartaric acids and sodium bicarbonate.

Formula

Two acids are used to avoid crumbling of the granules. Wet methods, dry methods, fusion methods, hot-melt extrusion methods and non-aqueous procedures are all viable options for producing effervescent granules.

Requirements: Sodium bicarbonate, citric acid, tartaric acid, anhydrous sodium carbonate, sodium saccharin, analytical balance, mortar and pestle, butter paper, etc.

Ingredients	Standard formula
Sodium bicarbonate	3.5 gm
Citric acid	2.5 gm
Tartaric acid	1.5 gm
Sodium saccharin	0.3 gm
Anhydrous sodium carbonate	2.5 gm
6b	1.5 gm

Procedure

1. Made the fine powders of all the ingredients and then passed them through sieve No. 60.
2. Weighed sodium carbonate, tartaric acid, anhydrous sodium carbonate and 6bseparately as required, transferred citric acid to mortar and mixed well.
3. Anhydrous sodium carbonate was added.
4. Add sodium saccharin added and mixed well.
5. Dried it in the oven.

Category: To decrease blood uric acid.

Storage: Kept in a sealed container and refrigerated.

Quality control studies of the prepared granules:

Assessment of 6b content

The 6b concentration was determined by added 200 mg of the granules by weight to 200ml of phosphate buffer solution (pH 6.8), mixed thoroughly, filtered and analyzed the solution with a UV-Visible spectrophotometer at 261 nm.

Flow-ability study

Both tapped density (TD) and bulk density (BD) were calculated as follow, certain amount of granules was weighted and transferred to a 100 ml measuring cylinder, after making any necessary corrections to the initial volume and recording the results, the measuring cylinder was tapped at a height of 2.5 cm every two seconds until the volume was stabilized. We applied the provided equation to calculate both bulk and tapped density.

$$BD = \frac{\text{granules weight}}{\text{packing volume}}$$

$$TD = \frac{\text{granules weight}}{\text{tapped volume of the packing}}$$

An important parameter was calculated to evaluate BD and TD which is Carr's index of 6b granules.

$$\text{Carrs index} = \frac{[(TD - BD) * 100]}{TD}$$

Table 1: Flow properties according to Carr's index

Flow characters	Carr's index
Excellent	1-10
Good	11-15
Fair	16-20
Passable	21-25
Poor	26-31
Very poor	32-37
Very, very poor	> 38

Then, the bellow equation was applied to calculate Hausner's ratio to emphasize good flowing properties of 6b granules. As standard ratios, ratios under 1.25 indicate excellent flowing capabilities, whereas ratios between 1.25 and 1.6 indicate only moderate flowing properties. On the other hand, more cohesive powders are indicated by a ratio greater than 1.6.

$$\text{Hausners ratio} = \frac{\text{tapped density}}{\text{bulk density}}$$

The angle of repose determination

The angle of repose can be used as a reliable measure for estimating the granular material's flow-ability. The employment of a funnel strategy. A conical pile is produced when granular materials are deposited over a flat surface. The angle of repose is defined as the vertical distance from the top of the pile to the ground. Tan of the angle of repose was calculated using the base cone diameter (D) and the height (H) of the cone. The following formula was used to calculate the angle of repose:

$$\text{Tan}\,\theta = \frac{H}{0.5 * D}$$

Table 2: Flowability properties according to angle of repose

The angle repose value	Flow properties
<20	Excellent
20-30	Good
30-34	Passable
>40	Very poor

Effervescence time

The effervescent time will be recorded after 200 mg of 6b granules have been added to 250 ml of water and stirred until a clear solution is achieved (table 3). Result: 92 seconds.

STATISTICAL ANALYSIS

Data in this study were expressed as the mean. Statistical analyses were performed by one-way ANOVA (analysis of variance) Sigma Plot software (SPSS Inc., Chicago, USA).

RESULTS

Anti-xanthine oxidase activity

The results had shown that black seed extract and compound 6b had promising activity 0.63µg/ml compared to Allupurinol 0.63µg/ml and other triazolopyrimidine derivatives had variable moderate activity other pyrimidine derivatives were inactive. The synergistic activity of both black seed extract and compound 6b was studied (table 4).

Docking study

The most effective compounds were designed in MOE 2014.09 and stored in a molecular databank (Ulc CCG., 2018). Protein Data Bank provided the crystal structure of xanthine dehydrogenase (PDB: 1n5x; resolution: 2.80Å) bound to febuxostat (ID: TEI; Protein 3D protonation and energy minimization were achieved with the help of MOE's structure preparation module. To prepare the crystal structure for docking, the ligand and water molecules were first removed. Rigid receptor was used as the docking methodology and the triangle matcher was used for placement, to identify the docking site and dock the database of all the investigated compounds. The rescoring functions London dG and GBVI/WSA dG were chosen, with force field employed for further modification. Only the highest-scoring position for each molecule was obtained after calculating the free binding energy (kcal/mol). The docked pose with the greatest docking score is regarded as the most likely binding configuration of the ligand for a given ligand and binding site.

In general, the binding profile of 6a-c with residues in the binding pocket indicates that these three compounds have

been appropriately located in the pocket and are well stabilized by several preferable electrostatic interactions. Enzyme interacts primarily by π–π, π–σ, π–alkyl, alkyl, carbon-hydrogen and distinctive hydrogen bonding. This is indicated by the fact that the overall pattern is as follows: The triazolopyrimidine moiety is covered by five hydrophobic residues (Phe914, Phe1009, Ala1078, Ala1079 and Val1011) and three hydrophilic residues (Glu802, Arg880 and Thr1010) respectively (fig.4).

The three compounds 6a-c docked into the active site and preserves the essential interaction, just like the crystalline molecule (febuxostat). The triazolopyrimidine ring participates in both π–π stacking interactions with Phe914 and Phe1009. Two H-bond interactions have been detected between the carbonyl function group of the triazolopyrimidone moiety (H-bond acceptor) and the highly basic guanidine group of Arg880. Comparable to febuxostat's carboxylate, as identified via its three-dimensional structure. Furthermore, cyanide substitution interacts via H bonds with Thr1010 and Val1011. As a final step, Glu802 forms a bi-dentate H-bond with the two nitrogen atoms (one a donor and the other an acceptor) in the triazolopyrimidine moiety. All of the bond distance was calculated from data collected from 3D models (fig. 4) and summarized at (table 5). Overall, the analysis reveals that the scaffold formed by the compounds 6a-c is the best option for inhibiting xanthine oxidase because it is well adorned with tiny, stiff and planar groups.

DISCUSSION

Chemistry

On the synthetic view, some new pyrimidines were prepared in light of knowledge of Biginelly one pot cyclo-condensation of thiourea 1, ethylcyanoacetate 2 and three aromatic aldehydes 3a-c in sodium ethoxide to give thiouracils 4a-c (Scheme 1). IR spectrum of compound 4a showed absorption bands at 3319, 3234 (2NH`s), 2220 (CN), 1683 (C=O) and 1277 (C=S) $cm^{-1}$. $^1H$ NMR spectrum showed a multiplet signals in the region at: δ = 7.59-8.06 ppm corresponding to the thiazole protons and a broad two singlet signal at: δ = 10.06, 11.15 ppm exchangeable with $D_2O$ for 2NH`s protons. The mass spectrum revealed a molecular ion peak at m/z 236. An acceptable mechanism (Mosaad *et al*. 2011) involves base catalysed condensation of the aldehyde and ethyl cyanoacetate (fig.3) yielding active arylidenes followed by Michael addition on active arylidenes forming 6-aryl-5-cyano-5,6-dihydro-2-thiouracils which were easily oxidized by atmospheric or thermal oxidations to give target compounds 4a-c. Hydrazinolysis of 4a-c by refluxing in hydrazine hydrate till all H_2S vapours were completely vanished afford hydrazinopyrimidines 5a-c. The structures of compounds 5a-c were in agreement with spectral and analytical data. For example, IR-spectra of 5a lacked thione (C=S) peak and appearance of a very broad peak for (NH_2) at 2320 cm^{-1} in addition the appearance of signal at δ 8.37 ppm in ^1H NMR spectrum corresponding to NH_2 group. Compounds 5a-c were cyclo-condensed with formic acid to yield triazolopyrimidines 6a-c which were confirmed by their chemical microanalyses and spectroscopic analyses, IR, NMR, and mass spectra.

4-Oxo-6-(thiazol-2-yl)-2-thioxo-1,2,3,4-tetrahydropyrimidine-5-carbonitrile (4a)

White solid, Yield: 73%: m.p 260-262ºC: IR ($\bar{\upsilon}_{max}$, cm^{-1}): 3319, 3234 (amino-H), 3176 (CH, aromatic), 2220 (cyano), 1683(carbonyl), 1277 (thione) cm^{-1}. ^1H NMR (500.1 MHz, DMSO-d_6): δ 7.59-8.06 (m, 2H, thiazole H), 10.06, 11.15 (2s, 2NH, D_2O exchangeable) ppm. ^{13}C NMR (125 MHz, DMSO-d_6): 89.06, 89.44, 125.41, 125.81, 139.03, 151.79, 152.22, 153.11, 169.41, 175.83ppm. MS (EI 70 eV): m/z (%)=236 [M^+]. Anal. Calculated for $C_8H_4N_4OS_2$ (236.27): C, 40.67; H, 1.71; N, 23.71. Found: C, 40.33; H, 1.66; N, 23.64.

4-Oxo-6-(6-(thiophen-3-yl)pyridin-2-yl)-2-thioxo-1,2,3,4-tetrahydropyrimidine-5-carbonitrile (4b)

White solid, Yield: 70%: m.p 275-277ºC: IR ($\bar{\upsilon}_{max}$,cm^{-1}):3340, 3237 (amino-H), 3185(CH, aromatic), 2225 (cyano), 1687 (carbonyl), 1270 (thione (cm^{-1}. ^1H NMR (500.1 MHz, DMSO-d_6): δ 7.52-8.2 (m, 6H, aromatic H), 9.28,10.28 (2s, 2NH, D_2O exchangeable) ppm. ^{13}C NMR (125 MHz, DMSO-d_6): 94.96, 111.04, 120.54, 122.85, 128.15, 129.44, 131.98, 133.56, 139.43, 150.82, 156.63, 157.04, 157.12, 177.56 ppm.MS (EI 70 eV): m/z (%)=312 [M^+]. Anal. Calculated for $C_{14}H_8N_4OS_2$ (312.37): C, 53.83; H, 2.58; N, 17.94. Found: C, 53.9; H, 2.43; N, 17.83.

4-Oxo-6-(thiazol-4-yl)-2-thioxo-1,2,3,4-tetrahydropyrimidine-5-carbonitrile (4c)

White solid, Yield: 81%: m.p 287-289ºC: IR ($\bar{\upsilon}_{max}$, cm^{-1}): 3359, 3239 (NH), 3165 (CH, aromatic), 2228 (cyano), 1688(carbonyl), 1271(thione) cm^{-1}. ^1H NMR (500.1 MHz, DMSO-d_6):δ7.94, 7.96 (2s, 2H, thiazole), 9.29, 10.47 (2s, 2H, 2NH, D_2O exchangeable) ppm.^{13}C NMR (125 MHz, DMSO-d_6): 98.48, 115.45, 120.89, 135.81, 138.11, 143.83, 152.98, 161.58, 171.98 ppm. MS (EI 70 eV): m/z (%)=236 [M^+]. Anal. Calculated for $C_8H_4N_4OS_2$ (236.27): C, 40.67; H, 1.71; N, 23.71. Found: C, 40.61; H, 1.67; N, 23.69.

2-Hydrazinyl-4-oxo-6-(thiazol-2-yl)-1,4-dihydropyrimidine-5-carbonitrile (5a)

White solid, Yield: 65%: m.p 300-302ºC: IR ($\bar{\upsilon}_{max}$, cm^{-1}): 3259, 2320 (2NH, NH_2), 3163 (CH, aromatic), 2230 (cyano), 1680 (carbonyl) cm^{-1}. ^1H NMR (500.1 MHz, DMSO-d_6): δ 7.54-8.04 (m, 2H, thiazole H), 8.37, 8.48, 9.00 (3s, 4H, 2NH`s &NH_2, D_2O exchangeable) ppm. ^{13}C NMR (125 MHz, DMSO-d_6): 103.74, 114.77, 120.77, 145.12, 155.12, 155.45, 156.84, 162.20, 175.78 ppm. MS (EI 70 eV): m/z (%)=234 [M^+]. Elemental analysis: Calculated for $C_8H_6N_6OS$ (234.24): C, 41.02; H, 2.58; N, 35.88. Found: C, 41.13; H, 2.59; N, 35.78.

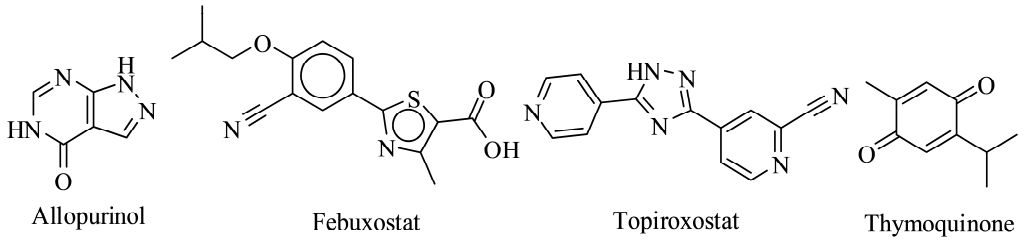

Fig. 1: FDA approved drugs as xanthine oxidase inhibitor.

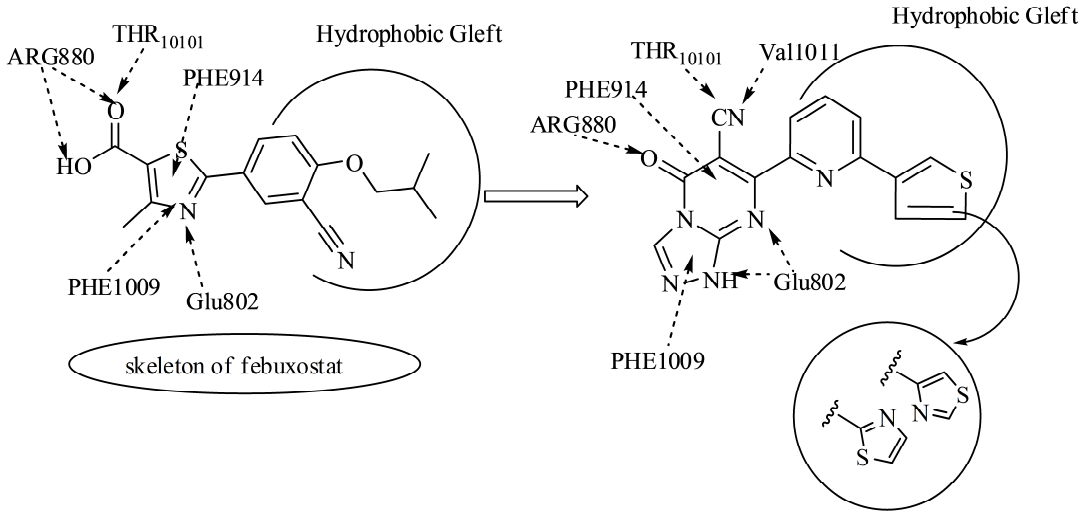

Fig. 2: Rational strategy: (a) relationship between the skeleton of febuxostat and the residues found at its binding pocket; (relationship between interactions of the novel designed molecules and febuxostat at the binding pocket.

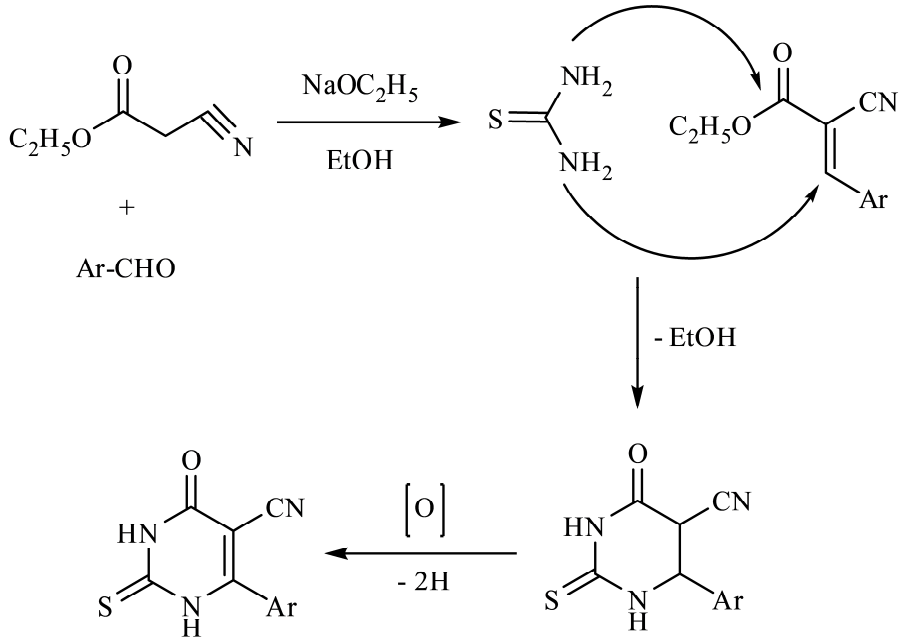

Fig. 3: Reaction mechanism of 6-aryl-5-cyano-5,6-dihydro-2-thiouracils formation.

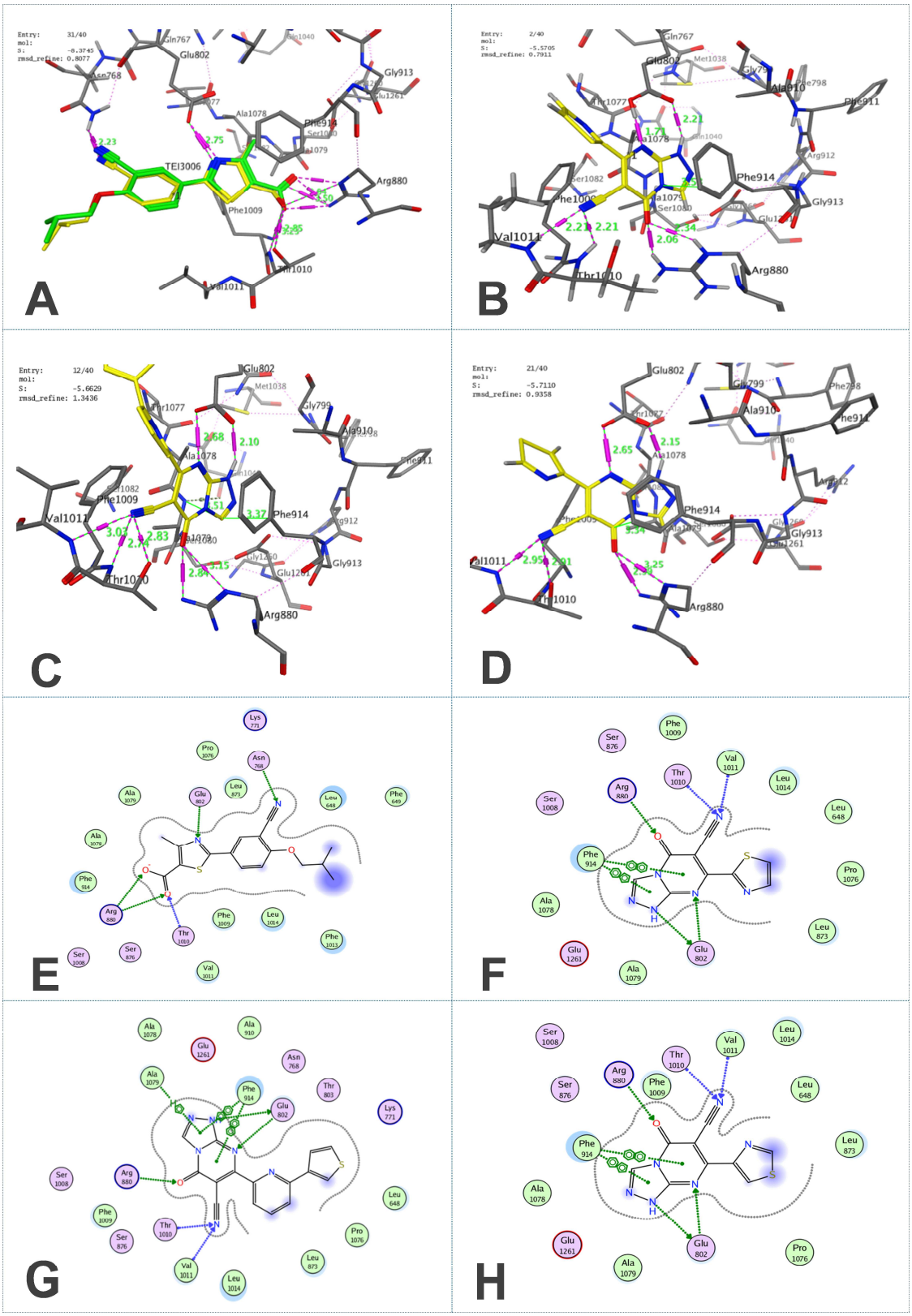

Fig. 4: A) Validation protocol: overlay of the co-crystallized ligand (green) and the redockedcrystallized ligand febuxostat (yellow) into the xanthine dehydrogenase (PDB entry: 1N5X)B)C) and D)3D structureof interactions of 6a-cwith residues of febuxostat binding pocket, respectively. E)F) G)andH)twodimensional structure showed interactions of febuxostatand6a-c with residues of binding site, respectively.

Table 3: Flow properties of 6b effervescent granules.

Flow property	Hausner's ratio	Carr's index	Angle of repose	Tapped density	Bulk density
Good	1.15	14	25	0.55	0.51

From table 3 granules of compound 6b showed good flow properties.

Table 4: Results of residual XO activity and IC_{50}% values of the black seed extract and synthesized compounds.

Compound	Residual XO activity (%) (60µg/ml)	IC_{50} (µg/ml)
Control	100	-
4a	13.87	18.98
4b	11.84	22.65
4c	13.23	20.46
5a	19.12	21.24
5b	14.72	19.71
5c	15.79	23.12
6a	4.12	5.62
6b	2.15	0.63
6c	4.87	4.84
Black seed extract	5.78	1.87
Black seed + 6b	2.23	0.60
Allupurinol (7.81µg/ml)	2.19	0.62

Table 5: Results of molecular docking of the crystallized ligand and most active compounds versus (PDBID: 1N5X).

Compoud No.	Score Kcal/mol	Rmsd (Å)	E score1 Kcal/mol	E score2 Kcal/mol	Binding interaction (Receptor-Ligand)
6a	-5.5705	0.7911	-12.1466	-5.7288	Glu 802-(triazolopyrimidine)= 1.71, 2.21 Å Arg 880-(C=O Pyrimidine) 2.06, 2.34 Å Phe 914-(triazolopyrimidine) ~ 3.53 Å Thr 1010-(CN)= 2.21 Å Val 1011-(CN)= 2.21 Å
6b	-6.2322	0.6802	-14.293	-6.23224	Glu 802-(triazolopyrimidine)= 2.10,2.68 Å Arg 880-(C=O Pyrimidine) = 2.84, 3.15 Å Phe 914-(triazolopyrimidine) ~ 3.52 Å Phe 914 ~ 3.37 Å Thr 1010-(CN)= 2.74, 2.83 Å Val 1011-(CN)= 3.03 Å
6c	-5.7110	0.9358	-11.7648	-5.71104	Glu 802-(triazolopyrimidine)= 2.65 ,2.15 Å Arg 880-(C=O Pyrimidine) = 2.99, 3.25 Å Phe 914-(triazolopyrimidine) ~ 3.34 Å Thr 1010-(CN)= 2.91 Å Val 101-(CN)= 2.95 Å Asn 768= 2.23 Å
Febuxostat (co-crystallized molecule)	-8.3745	0.8077	-12.6402	-8.37451	Glu 802= 1.71, 2.21 Å Arg 880-(C=O Pyrimidine) = 2.06, 2.34 Å Thr 1010= 2.21 Å

2-Hydrazinyl-4-oxo-6-(6-(thiophen-3-yl)pyridin-2-yl)-1,4-dihydropyrimidine-5-carbonitrile (5b)

White solid, Yield: 67%: m.p 310-312°C: IR ($\bar{\upsilon}_{max}$, cm^{-1}): 3434, 3258, 2210 (2NH, NH_2), 3164 (CH, aromatic), 2235 (cyano), 1683 (carbonyl) cm^{-1}. ^1H NMR (500.1 MHz, DMSO-d_6): δ 7.59-8.40 (m, 6H, aromatic H), 8.50, 9.48, 10.53 (3s, 4H, 2NH`s &NH_2, D_2O exchangeable) ppm. ^{13}C NMR (125 MHz, DMSO-d_6): 101.20, 114.79, 120.78, 125.72, 126.46, 127.17, 127.92, 128.19, 128.73, 128.84, 128.94, 130.19, 148.51, 152.22, 162.39 ppm. MS (EI 70 eV): m/z (%)=310[M^+]. Elemental analysis: Calculated for $C_{14}H_{10}N_6OS$ (310.33): C, 54.18; H, 3.25; N, 27.08. Found: C, 54.21; H, 3.39; N, 27.07.

2-Hydrazinyl-4-oxo-6-(thiazol-4-yl)-1,4-dihydropyrimidine-5-carbonitrile(5c)

White solid, Yield: 62%: m.p 305-307°C: IR ($\bar{\upsilon}_{max}$, cm^{-1}): 3440, 3267, 2335 (2NH, NH_2), 3164 (CH, aromatic), 2235 (cyano), 1682 (carbonyl) cm^{-1}. ^1H NMR (500.1 MHz, DMSO-d_6): δ 6.61 (br.s, 2H, NH_2, D_2O

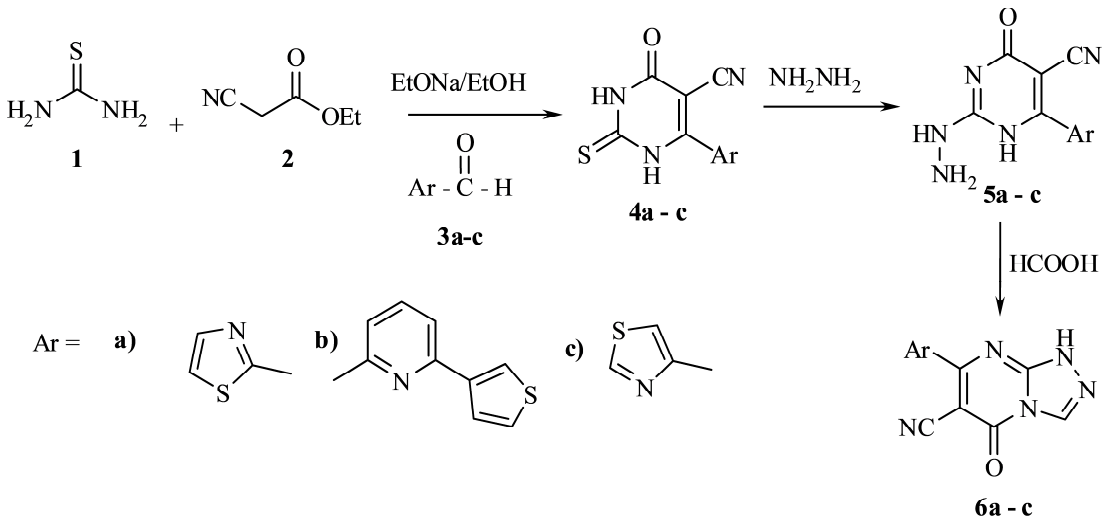

Scheme 1: Synthesis of pyrimidine and triazolopyrimidine derivatives.

exchangeable), 7.66, 8.28 (2s, 2H, thiazole H), 9.11, 10.61 (2s, 2NH`s, D_2O exchangeable) ppm.^{13}C NMR (125 MHz, DMSO-d_6): 80.13, 113.62, 116.36, 140.86, 153.86, 156.42, 156.66, 163.21ppm. MS (EI 70 eV): m/z (%)=234[M^+]. Elemental analysis: Calculated for $C_8H_6N_6OS$ (234.24): C, 41.02; H, 2.58; N, 35.88. Found: C, 41.11; H, 2.09; N, 35.73.

5-Oxo-7-(thiazol-2-yl)-1,5-dihydro-[1,2,4]triazolo[4,3-a]pyrimidine-6-carbonitrile (6a)

White solid, Yield: 67%: m.p 317-319^{o}C: IR (ῡ$_{max}$, cm^{-1}): 3249 (NH), 3177 (CH, aromatic), 2223 (cyano), 1689(carbonyl) cm^{-1}. ^{1}H NMR (500.1 MHz, DMSO-d_6): δ 7.59, 8.92 (2d, 2H, thiazole H), 9.90 (s, 1H, triazole H) 11.29 (s, 1H, NH, D_2O exchangeable) ppm. ^{13}C NMR (125 MHz, DMSO-d_6): 95.75, 118.06, 120.75, 124.04, 144.22, 152.20, 153.29, 154.01, 175.79 ppm. MS (EI 70 eV): m/z (%)=244[M^+]. Elemental analysis: Calculated for $C_9H_4N_6OS$ (244.23): C, 44.26; H, 1.65; N, 34.41. Found: C, 44.18; H, 1.72; N, 34.53.

5-Oxo-7-(6-(thiophen-3-yl)pyridin-2-yl)-1,5-dihydro-[1,2,4]triazolo[4,3-a]pyrimidine-6-carbonitrile (6b)

White solid, Yield: 63%: m.p 311-313^{o}C: IR (ῡ$_{max}$, cm^{-1}): 3282 (NH), 3196 (CH aromatic), 2227 (cyano), 1679 (carbonyl) cm^{-1}. ^{1}H NMR (500.1 MHz, DMSO-d_6): δ 7.59-8.51 (m, 6H, aromatic H), 9.48 (s, 1H, triazole H), 10.08 (s, 1H, NH, D_2O exchangeable) ppm. ^{13}C NMR (125 MHz, DMSO-d_6): 93.68, 117.74, 121.95, 122.75, 123.45, 128.14, 131.96, 133.90, 138.14, 138.27, 148.15, 153.28, 155.45, 157.65, 159.44 ppm. MS (EI 70 eV): m/z (%)=320[M^+]. Elemental analysis: Calculated for $C_{15}H_8N_6OS$ (320. 33): C, 56.24; H, 2.52; N, 26.24. Found: C, 56.38; H, 2.45; N, 26.19.

5-Oxo-7-(thiazol-4-yl)-1,5-dihydro-[1,2,4]triazolo[4,3-a]pyrimidine-6-carbonitrile (6c)

White solid, Yield: 65%: m.p 309-311^{o}C: IR (ῡ$_{max}$, cm^{-1}): 3251 (NH), 3172 (CH aromatic), 2219 (cyano), 1681 (carbonyl) cm^{-1}. ^{1}H NMR (500.1 MHz, DMSO-d_6): δ 7.59, 8.05 (2s, 2H, thiazole H), 9.25 (s, 1H, triazole H), 10.32 (s, 1H, NH, D_2O exchangeable) ppm. ^{13}C NMR (125 MHz, DMSO-d_6): 100.00, 115.27, 120.69, 125.13, 138.16, 139.66, 150.11, 153.11, 157.72, 171.61 ppm. MS (EI 70 eV): m/z (%)=244[M^+].Elemental analysis: Calculated for $C_9H_4N_6OS$ (244.23): C, 44.26; H, 1.65; N, 34.41. Found: C, 44.23; H, 1.58; N, 34.51.

In vitro-antixanthine oxidase activity:

The inhibitory activity of xanthine oxidase of black seed extract and various prepared compounds was measured spectrophotometrically at 296 nm results were evaluated using standard deviation calculations and by IC_{50} determination using allupurinol as a reference standard.

Formulation

Compound 6b was formulated as effervescent granules using a balanced formula of citric acid, tartaric acid and sodium bicarbonate. Granules were subjected to quality control studies especially flowability study (table 3) and evaluated according to Carr 's index for 6b granules also, angle of repose was determined in addition to effervescence time.

Molecular modelling

The objectives of this research was to use molecular modelling to better comprehend the intricate framework of molecular interactions responsible for the inhibitory effect of the most potent xanthine oxidase inhibitor, 6a-c. The X-ray crystallographic structure of xanthine dehydrogenase complexed with lead compound, febuxostat (PDB entry: 1N5X; resolution: 2.80) was utilized for this particular objective (Okamoto *et al*., 2003).

To validate the docking protocol, the ligand febuxostat was co-crystallized with the protein and then docked into its binding site. The credibility of the docking

methodology was demonstrated by the fact that the algorithm was able to generate the best fit confirmation of febuxostat in chain A with a root mean square deviation (RMSD) value of 0.8077 and a binding affinity of -8.3745 kcal/mol (fig. 4A). After that 6a-c was docked into the binding site, multiple docked conformations of were created and each one was ranked according to the in silico binding affinity that it possessed. The conformation that had the highest binding affinity was chosen for discussion and the data from the poses that had the highest binding affinity were chosen for discussion and summarized.

CONCLUSION

All synthesized compounds were evaluated as xanthine oxidase inhibitors. Non condensed pyrimidines4a-c and 5a-c showed weak activity, while triazolopyrimidines showed moderate activity except compound 6b that showed potent and comparable activity relative to allupurinol which was used as a reference standard drug. Compound 6b was formulated as effervescent granules and showed good flow ability properties. In silico docking studies showed that febuxostat bind at target binding pocket and maintain the crucial interaction with the key amino acids.

REFERENCES

Abdizadeh R, Heidarian E, Hadizadeh F and Tooba A (2020). Investigation of pyrimidine analogues as xanthine oxidase inhibitors to treat of hyperuricemia and gout through combined QSAR techniques, molecular docking and molecular dynamics simulations. *J. Taiwan Inst. Chem. Eng*., **113**: 72-100.

Abedi AS, Rismanchi M, Shahdoostkhany M, Mohammadi A and Mortazavian AM (2017). Microwave-assisted extraction of *Nigella sativa* essential oil and evaluation of its antioxidant activity. *J. Food Sci. Technol*., **54**(12): 3779-3790.

Ahmad, A, Husain A, Mujeeb M, Khan SA, Najmi AK, Siddique NA, Damanhouri ZA and Anwar F (2013). A review ontherapeutic potential of *Nigella sativa*: A miracle herb. *Asian Pac. J. Trop. Biomed*, **3**(5): 337-352.

Ahmad R, Ahmad N and Shehzad A (2020). Solvent and temperature effects of accelerated solvent extraction (ASE) coupled with ultra-high pressure liquid chromatography (UHPLC-DAD) technique for determination of thymoquinone in commercial food samples of black seeds (Nigella sativa) *Food Chem*., **30**(309): 125740.

Al-Mousawy H, Al-Hussainy Z and Al-aayedi M (2019). Formulation and evaluation of effervescent granules of Ibuprofen. *Int. J. Pharm.,* **11**(6): 66-69.

Battelli MG, Polito L, Bortolotti M and Bolognesi A (2016). Xanthine oxidoreductase-derived reactive species: physiological and pathological effects. *Oxid. Med. Cell. Longev*, **2016**: 1-8.

Cobourne-Duval MK, Taka E, Mendonca P and Soliman KFA (2018).Thymoquinone increases the expression of neuroprotective proteins while decreasing the expression of pro-inflammatory cytokines and the gene expression NF_B pathway signaling targets in LPS/IFN -activated BV-2 microglia cells. *J. Neuroimmunol*, **320**: 87-97.

Dinagaran S, Sridhar S and Eganathan P (2016). Chemical composition and antioxidant activities of black seed oil (*Nigella sativa*). *Int. J. Pharm. Sci. Res*., **7**(11): 4473-4479.

Dzobo K (2022). The Role of natural products as sources of therapeutic agents for innovative drug discovery. *Comprehensive Pharmacol.*, **2**: 408-22.

Enroth C, Eger BT, Okamoto K, Tomoko N, Takeshi N and Emil FP (2000). Crystal structures of bovine milk xanthine dehydrogenase and xanthine oxidase: structure-based mechanism of conversion. *PNAS*, **97**(20): 10723-10728.

Fathalla OA, Abd El-Hamid MA, Awad SM and Mohamed MS (2007). Synthesis of novel 2-thiouracil derivatives with analgesic, anti-inflammatory and antipyretic activities. *Egy. Pharm. J*., **6**(2): 153-163.

Habibeh M, Ramin R and Gholamreza K (2020). Nigella sativa safety: An overview. *Asian Biomed. Res*, **14**(4): 127-137.

Hammer B, Wagner AandBohm M (2001). Fatal allupurinol induced hypersensitivity syndrome in asymptomatic hyperuricaemia. *Dutsch. Med. Wochenschr*, **126**(47): 1331-1334.

Horiuchi H, Ohta M, Nishimura S, Kaneko H,Kasahara Y and Kornooriya K (2000). Allupurinol inducers renal toxicity by impairing pyrimidine metabolism in mice. *Life Sci*., **66**(21): 2051-2070.

Houghton PJ, Zarka R, de lasHeras B and Hoult JR (1995). Fixed oil of *Nigella sativa* and derived thymoquinone inhibit eicosanoidgeneration in leukocytes and membrane lipid peroxidation. *Planta Med*., **61**(1): 33-36.

Liu N, Xu H, Sun Q, Xiaojan Y, Wentong C, Hongguan W, Jie J, Youzhi X and Wenjie L (2021). The Role of oxidative Stress in hyperuricemia and xanthine oxidoreductase (XOR) inhibitors. *Oxid. Med. Cell. Longev*, **2021**: 1-15.

Jaarin K, Foong W, Yeoh M, Kamaraul Z, Qodriyah H and Azman A (2015). Mechanisms of the antihypertensive effects of *Nigella sativa* oil in L-NAME-induced hypertensive rats. *Clinics*, **70**(11): 751-757.

Kiralan M, Özkan G, Bayrak A and Ramadan MF (2014). Physicochemical properties and stability of black cumin (*Nigella sativa*) seed oil as affected by different extraction methods. *Indus. Crops Prod*., **57**: 52-58.

Kokoska L, Havlik J, Valterova I, Sovova H, Sajfrtova M and Jankovska I (2008). Comparison of chemical composition and antibacterial activity of *Nigella sativa*

seed essential oils obtained by different extraction methods. *J. Food Prot*., **71**(12): 2475-2480.

KootiW, Hasanzadeh-Noohi Z, Sharafi-Ahvazi N, Asadi-Samani M and Ashtary-Larky D (2016). Phytochemistry; pharmacology; andtherapeutic uses of black seed (*Nigella sativa*). *Chin. J. Nat. Med*., **14**(10): 732–745.

Moghimi M, Farzaneh V and Bakhshabadi H (2018). The effect of ultrasound pretreatment on some selected physicochemical properties of black cumin (*Nigella sativa*) *Nutrire*., **43**(1): 18.

Mohamed MS, Awad SM and Ahmed NM (2011).Synthesis and antimicrobial activities of new indolyl pyrimidine derivatives. *J. App. Pharm. Sci*., **1**(5): 76-80.

Mosaad SM, Samir MA and Naglaa MA (2011). Synthesis and antimicrobial evaluation of some 6-aryl-5-cyano-2-thiouracil derivatives. *Acta Pharm*., **61**(2): 171-185.

Ojha R, Singh J, Ojha A, HarbinderS,SahilS and Kunal N (2017)An updated patent review: Xanthine oxidase inhibitors for the treatment of hyperuricemia and gout (2011-2015). *Expert Opin. Ther. Pat*., **27**(3):311-345.

Okamoto K, Eger BT, Nishino T, Kondo S, Pai EF and Nishino T (2003).An extremely potent inhibitor of xanthine oxidoreductase. Crystal structure of the enzyme-inhibitor complex and mechanism of inhibition. *J Biol Chem*., **278**(3):1848-55.

Okamoto K, Kusano T and Nishino T (2013). Chemical nature and reaction mechanisms of the molybdenum cofactor of xanthine oxidoreductase. *Curr. Pharm. Des*, **19**(14): 2606-2614.

Patel B, Suhagia B, Tejas B and Tushar R (2016). Preparation and evaluation of effervescent tablets of Ibuprofen. *Wo. J. Pharmacy. Pharm. Sci*., **2**(4): 2145-2155.

Razavi B and Hosseinzadeh H (2014). A review of the effect of Nigella sativa and its constituents in metabolic syndrome. *J. Endocri. Invest*., **37**(11): 1031-1040.

Sabriu-Haxhijaha A, Popovska O and Mustafa Z (2020).Thin-Layer chromatography analysis of *Nigella sativa* essential oil. *J. Hyg. Eng. Des*., **31**: 152-156.

Samarghandian S, Farkhondeh T and Samini F (2018). A Review on possible therapeutic effect of *Nigella sativa* and thymoquinone in neurodegenerative diseases CNS neurol. *Disord. Drug Targets*, **17**(6): 412-420

Trunghu B, Nguyen N and Xuan H (2016). Design and synthesis of chalcone derivatives as potential non-purine xanthine oxidase inhibitors. *Springerplus*, **5**(1): 1789-1795.

ULC, C. C. G. (2018). Molecular Operating Environment (MOE), 2013.08. 1010 Sherbooke St. West, Suite# 910, Montreal, QC, Canada, H3A 2R7, 10.

Wang L, Weller C, Schlegel V, Carr T and Cuppett S (2008). Supercritical CO_2 extraction of lipids from grain sorghum dried distillers grains with solubles. *Bioresour Technol*, **99**(5): 1373-82.

Zielińska M, Dereń K, Polak-Szczybyło E andStępień AE (2021). The role of bioactive compounds of *Nigella sativa* in rheumatoid arthritis therapy-current reports. *Nutrients*, **13**(10): 3369.